

Photoreflectance of r.f. sputtered $\text{Cd}_{1-x}\text{Fe}_x\text{Te}$ thin films

C. VÁZQUEZ-LÓPEZ*, F. CERDEIRA

Instituto de Física "Gleb Wataghin", UNICAMP, Caixa Postal 6165, 13081-Campinas S.P., Brazil

F. SÁNCHEZ-SINENCIO, J. G. MENDOZA-ALVAREZ

Depto. de Física, Centro de Investigación del IPN, Apdo. Postal 14-740, México 07000, D.F.

OCTAVIO ALVAREZ-F.

Instituto de Investigación en Materiales, UNAM, México, D.F.

Samples of r.f. sputtered $\text{Cd}_{1-x}\text{Fe}_x\text{Te}$ (with $x = 0.00, 0.05, 0.10$ and 0.15) films were studied by photoreflectance spectroscopy. The samples were grown at a substrate temperature of 150°C . The photoreflectance spectra around the fundamental edge were analysed using the generalized theory of electroreflectance in the low-field regime recently developed by Raccach *et al.* The experimental results for $x = 0.00$ and 0.05 show a single feature that can be interpreted in terms of optical transitions in a cubic phase structure. In those films where $x = 0.10$ and 0.15 , the experimental results show a double feature spectrum that we attribute to optical transitions in an hexagonal phase structure. Subsequent annealing at 200 and 300°C of the samples produces some changes in the lineshape of the photoreflectance spectra. These changes are interpreted in terms of an increment in the density of polarizable defects as the annealing temperature increases; we associate this effect with an increase in the formation of complex defects composed of Fe^{3+} ions and cadmium vacancies.

1. Introduction

Structural, electrical, magnetic and optical properties of semiconductors formed from II-VI compounds with a controlled quantity of magnetic ions, have been widely investigated, mainly on single-crystal compounds [1-3]. Less extensive studies have been made on these semiconductors in the form of polycrystalline and/or amorphous films [4, 5]. On the other hand, a study of ternary compounds can be useful in understanding the process of impurification of the host material. In particular, CdTe thin films have a broad range of technological applications [6], but their use for building actual devices is limited by the present lack of understanding of the role of impurities in the doping process. Several experimental techniques have been used in the study of doping and defect structure of this semiconductor [4, 5, 7]. In this work, photoreflectance spectroscopy (PR) has been used. This is a contactless form of modulation in which the optical constants are modulated by periodically decreasing the built-in field in the material by the photogeneration of electron-hole pairs [8]. Such a modulation produces rich spectral features in the vicinity of critical points [9], leading to the determination of interband transition energies in semiconductors. Also, as for the case of electroreflectance (ER) [10], the possibility of an interaction between the built-in modulating field and the defects extends the

applicability of the attractively simple PR technique to the study of defects in semiconductors. We have studied the evolution of the PR fundamental optical transition of $\text{Cd}_{1-x}\text{Fe}_x\text{Te}$ polycrystalline films for iron compositions in the range from 0% to 15%, as a function of isochronal thermal annealing at different temperatures.

2. Experimental details

$\text{Cd}_{1-x}\text{Fe}_x\text{Te}$ thin films were grown in a diode r.f. sputtering system, as reported by Fragoso *et al.* [11]. The target to substrate distance was 3 cm. A target of 1 cm diameter, mounted on an air-cooled cathode, was made by vacuum pressing 99.999% pure CdTe powder from Cerac Inc. together with a piece of iron foil, whose area was in accordance with the desired iron concentration. The films were grown on Corning 7059 glass substrates. Prior to film growth the chamber was evacuated at a pressure of 3×10^{-6} torr. Argon of 99.999% purity was used in the sputtering process. Just before deposition, the target was usually presputtered for 15 min under growth conditions. During the deposition the pumping speed was throttled. The samples were grown at a substrate temperature of 150°C , and the time of deposition was 60 min under an argon pressure of 3 m torr. A SAM-ESCA system was used to determine the iron concentration in the films and to verify that there were

*On leave from the Instituto de Ciencias de la Universidad Autónoma de Puebla.

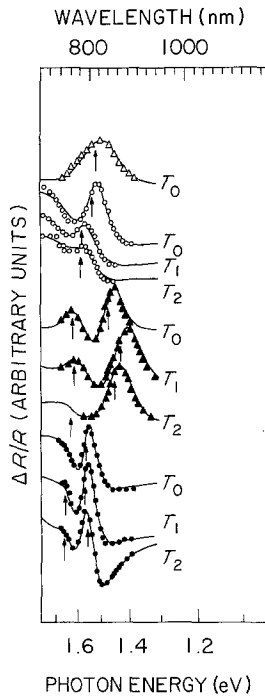


Figure 1 Room-temperature photorefectance spectra of $\text{Cd}_{1-x}\text{Fe}_x\text{Te}$ for various iron concentrations and three annealing temperatures: T_0 (not annealed), T_1 (annealed at 200°C), and T_2 (annealed at 300°C). The continuous curves are the results of least square fittings to the expression given in Equation 1. (Δ) $x = 0.00$, (\circ) $x = 0.05$, (\blacktriangle) $x = 0.10$, (\bullet) $x = 0.15$.

no iron clusters. The sample thickness, determined with a Dektak Sloan profile analyser, was on average $10\ \mu\text{m}$.

The PR spectra were obtained at room temperature using standard optical and phase-sensitive techniques as described previously [12]. The PR signals were proportional to the modulating intensity of the laser beam.

3. Results and discussion

Fig. 1 shows the experimental results of PR for the samples specified in the first two columns of Table I. In order to analyse these spectra, we used the low-field limit generalized theory of electroreflectance (ER) developed by Raccach *et al.* [10]. The generalized functional form of ER for the E_0 critical point can be

written as

$$L(E) = H_1\Gamma^{2.5}L(E, 5/2) - H_2\Gamma^{1.5}L(E, 3/2) - H_3\Gamma^{0.5}L(E, 1/2) \quad (1)$$

where

$$L(E, n/2) = [A/(E^2 + \Gamma^2)] \cos[\theta - n\phi(E)/2] \times [(E - E_0)^2 + \Gamma^2]^{-n/4} \quad (2)$$

with

$$\phi(E) = \tan^{-1}[\Gamma/(E - E_0)] \quad (3)$$

Here A , E_0 , Γ and θ are the amplitude, fundamental interband transition energy, phenomenological broadening parameter, and corresponding phase, respectively. The constants H_1 , H_2 and H_3 are merely scaling weighting factors. In each term of Equation 1 a $\Gamma^{n/2}$ factor has been introduced, to separate explicitly the dependence of the size of the PR lineshape from the Γ parameter.

The Raccach *et al.* parameters for the measurements of the polarizable defects are [13]

$$\Delta\sigma^2/(\hbar\Omega)^3 = H_2/(4\Gamma H_1) \quad (4)$$

and

$$\Delta E_0/(\hbar\Omega)^3 = H_3/(4\Gamma^2 H_1) \quad (5)$$

where $\Delta\sigma^2/(\hbar\Omega)^3$ and $\Delta E_0/(\hbar\Omega)^3$ are quantities proportional to the density of polarizable defects and to the density of polarizable inhomogeneous strains, respectively.

The most striking feature of Fig. 1 is that for values of $x \leq 0.05$ the PR spectrum can be fitted with only one optical transition, while for $x \geq 0.10$ two such transitions are necessary to fit the experimental data. The position of the optical gaps obtained from our fittings are indicated by arrows in Fig. 1 and shown schematically in the inset of Fig. 2. These gaps are not to be interpreted literally as the separation between the formerly degenerated valence bands, because the samples are probably composed of mixtures of zincblende and wurtzite structures.

Fig. 2 also shows the evolution of the parameter $\Delta\sigma^2/(\hbar\Omega)^3$ as a function of annealing temperature (T_A) for each value of iron concentration. First we notice that in samples with $x = 0.00$, $\Delta\sigma^2 = 0$ and $\Delta E_0 = 0$

TABLE I Parameters obtained from fitting Equation 1 to the experimental PR spectra

Sample	Temperature	A (10^{-6})	E_0 (eV)	θ	Γ (meV)	$\Delta\sigma^2/(\hbar\Omega)^3$ (eV^{-1})	$\Delta E_0/(\hbar\Omega)^3$ (eV^{-2})
CdTe	T_0	116	1.51	4	177	0	0
$\text{Cd}_{0.95}\text{Fe}_{0.05}\text{Te}$	T_0	71	1.57	4.7	81	0.62	-49.5
	T_1	32	1.57	4.7	96	0.65	-62.4
	T_2	0.84	1.57	4.7	96	1.69	-95.0
$\text{Cd}_{0.90}\text{Fe}_{0.10}\text{Te}$	T_0	12.8	1.47	4.7	80	0	0
		6.9	1.61	3.9	105	0	0
	T_1	34.6	1.43	4.7	110	0.45	-6.2
		12.0	1.60	4.3	110	0.45	-6.2
		1.6	1.45	4.7	100	1.10	-8.8
T_2	0.3	1.62	2.4	100	1.10	-8.8	
$\text{Cd}_{0.85}\text{Fe}_{0.15}\text{Te}$	T_0	146	1.56	5.0	58	0.87	-93
		43	1.56	4.9	63	1.67	-75
	T_1	5.2	1.64	3.9	62	1.68	-75
		1.7	1.54	3.9	65	1.62	-71
		0.25	1.64	3.9	65	1.62	-71

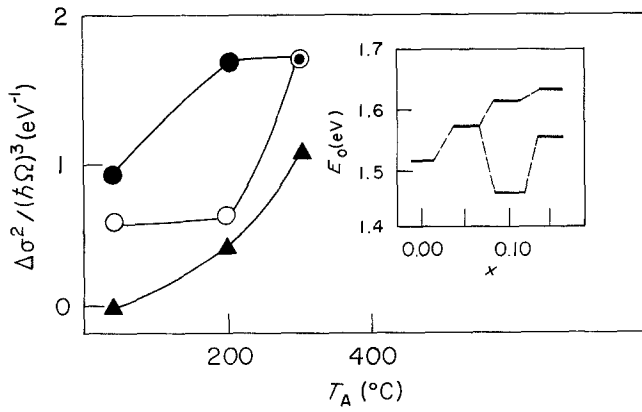


Figure 2 $\Delta\sigma^2/(\hbar\Omega)^3$, representing the density of polarizable defects, obtained from the fittings shown in Fig. 1 at different stages of annealing. The continuous lines are guides for the eye, only. The inset represents the behaviour of the fundamental band gap as a function of iron concentration. (O) $x = 0.05$, (\blacktriangle) $x = 0.10$, (\bullet) $x = 0.15$.

(see Table I), although the linewidth parameter, Γ , is larger than that corresponding to the other values of x . This probably means that in these samples we have very low density of polarizable defects ($\Delta\sigma^2 = 0$) and also of inhomogeneous strain ($\Delta E_0 = 0$), while the number of neutral defects is large, resulting in a large value of Γ .

As we go to the sample with $x = 0.05$, we observe (see Table I) that the data for the first spectrum (labelled T_0 to indicate samples which have not been annealed) are fitted with values of Γ which are about one half of those used in fitting the $x = 0.00$ sample. This suggests that some iron atoms have filled in the cadmium vacancies of the pure sample, thus diminishing the amount of neutral defects. In contrast, the amount of polarizable defects has reached a considerable proportion as shown by the large values of $\Delta\sigma^2$ (Table I).

Next we examine the evolution of these samples ($x = 0.05$) with the annealing temperature. In the annealing process the energy gap (E_0) and intrinsic linewidth (Γ) do not change significantly as T_A increases. On the other hand, the density of polarizable defects and of inhomogeneous strains seem to increase sharply with increasing annealing temperature, as evidenced by the corresponding increases in $\Delta\sigma^2$ and ΔE_0 . The evolution of these quantities as a function of T_A is shown in Figs 2 and 3, respectively. Mössbauer measurements performed in these samples [14] indicate that iron enters into the host material in two valence states: Fe^{2+} and Fe^{3+} , and that each Fe^{3+} ion is associated with a negatively charged cadmium vacancy. In this way, each Fe^{2+} ion could fill in a cadmium vacancy, which diminishes the number of neutral defects, while each Fe^{3+} ion would increase the density of polarizable defects and inhomogeneous strain. Thus, the increase in $\Delta\sigma^2$ and of ΔE_0 as T_A increases (Table I and Figs 2 and 3) observed in the $x = 0.05$ sample points to an increase in the $\text{Fe}^{3+}/\text{Fe}^{2+}$ ratio with increasing annealing temperature. This interpretation of our data is consistent with the results of Mössbauer spectroscopy [14].

The spectra corresponding to $x = 0.10$ and

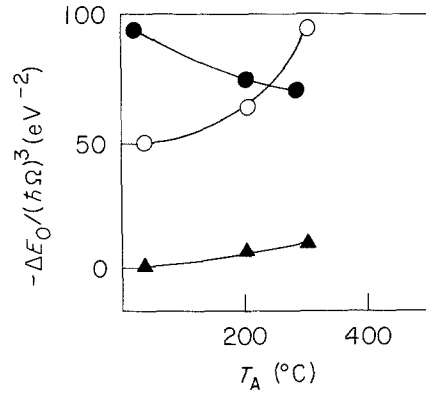


Figure 3 Parameter $\Delta E_0/(\hbar\Omega)^3$, representing the density of polarizable inhomogeneous strain, for various iron concentrations and annealing temperatures. The solid lines are guides for the eye. (O) $x = 0.05$, (\blacktriangle) $x = 0.10$, (\bullet) $x = 0.15$.

$x = 0.15$ can only be fitted assuming two closely spaced optical transitions which we attributed to a change in structure from zincblende to wurtzite, occurring at some concentration $0.05 < x < 0.10$. Such phase transition in this material is not very surprising. It has been reported that an excess of cadmium promotes the growth of the wurtzite structure in CdTe thin films, although the zincblende structure is the stable form for bulk CdTe ([6], p. 56). The fact that $\Delta\sigma^2/(\hbar\Omega)^3$ and $\Delta E_0/(\hbar\Omega)^3$ for the $x = 0.10$ samples are always lower than those corresponding to the $x = 0.05$ sample is consistent with this interpretation, because the strain that is built up in the latter type of sample by the inclusion of Fe^{3+} ions would be relieved by the structural change. As T_A increases, however, these quantities increase as they did in the other sample. Finally, for samples with $x = 0.15$ both the density of polarizable defects and of inhomogeneous strains go back to their previous high values (Table I), while the strain seems to relax slightly as T_A increases, consistent with our previous interpretation.

An alternative explanation for the observation of several optical transitions in the neighbourhood of the direct gap, is advanced by Joshi and Mogollón [15]. These authors, working with samples of very low iron concentration ($x < 0.05$) observe several weak structures at slightly higher energy than the fundamental absorption edge, which they attribute to transitions originating in core levels of the iron ions. These structures become progressively weaker as the iron concentration increases, so they may not be important at the higher concentrations that we report in our work. Also, their explanation would imply the observation of several structures and not merely the splitting of the E_0 transition into two distinct structures. Finally, the interpretation of Joshi and Mogollón does not explain the contributions of strain and polarizable defects to the PR lineshape. Hence, we believe that the interpretation given above, although tentative, gives a more coherent description of the observed photoreflectance behaviour.

In conclusion, the analysis of PR spectra for $\text{Cd}_{1-x}\text{Fe}_x\text{Te}$ leads to the following interpretation. For low iron concentrations, the structure of the

material is zinblende and iron ions enter in cadmium sites both as Fe^{2+} and as Fe^{3+} . The latter type of ion is associated with a negatively charged cadmium vacancy. As annealing temperature increases, more Fe^{2+} transforms into Fe^{3+} with consequent creation of new cadmium vacancies. As the concentration of the latter type of defect increases (with increasing x or T_A), strains build up and they are eventually released by a transition into the wurtzite structure. From this point on, increasing x or T_A results again in increasing the Fe^{3+} concentration with the resulting increase in polarizable defects. This interpretation is consistent with independent Mössbauer measurements. Electron microdiffraction spectroscopy should prove whether this zinblende to wurtzite structural transition really takes place at $0.05 < x < 0.10$. The above discussion shows that PR spectroscopy is a powerful, non-destructive, diagnostic tool in the study of semiconductors with a high density of defects.

Acknowledgements

This work has been partially supported by the Fundação de Amparo a Pesquisa do Estado de São Paulo (FAPESP). C.V.L. thanks FAPESP for a scholarship, and also acknowledges the IFGW-UNICAMP support through a "Bolsa Gleb Wataghin" in the initial stages of this work. We also acknowledge partial financial support of the Consejo Nacional de Ciencia y Tecnologia (CONACyT-México), the Organization of American States and the Fundación Ricardo J. Zevada/México. The help of Fausto de Camargo Jr in the least square fitting programme is also acknowledged.

References

1. J. A. GAJ, *J. Phys. Soc. Jpn* **49** Suppl. A. (1980) 797.
2. G. A. SLACK, S. ROBERTS and J. T. VALLIN, *Phys. Rev.* **189** (1969) 511.
3. R. R. GALAZKA, in Proceedings of the 14th Institute of Physics Conference, Series No. **43** (1979) 133.
4. K. LISCHKA, G. BRUNTHALER and W. JANTSCH, *J. Cryst. Growth* **72** (1982) 355.
5. L. F. SCHNEEMEYER, B. A. WILSON, W. P. LOWE, F. J. DI SALVO, S. E. SPENGLER, J. V. WASZCZAK and J. F. DILLON Jr, Materials Research Society 1986 Spring Meeting, Abstract Book, (NRS, Boston, 1986) p. 43.
6. K. ZANIO, "Semiconductors and Semimetals", Vol. 13 (Academic, New York, 1978).
7. G. BRUNTHALER, U. KAUFMANN and J. SCHNEIDER, *J. Appl. Phys.* **56** (1984) 2974.
8. D. E. ASPNES, *Solid State Commun.* **8** (1970) 267.
9. *Idem*, *Surf. Sci.* **37** (1973) 418.
10. PAUL M. RACCAH, J. W. GARLAND, Z. ZHANG, U. LEE, DA ZHONG XUE, L. L. ABELS, S. UGUR and W. WILINSKY, *Phys. Rev. Lett.* **53** (1984) 1958.
11. O. A. FRAGOSO, J. G. MENDOZA-ALVAREZ and F. SANCHEZ-SINENCIO, in "Lectures on Surface Science, edited by G. R. Castro and M. Cardona (Springer-Verlag, Berlin, Heidelberg, 1987) p. 52.
12. C. VAZQUEZ-LOPEZ, H. NAVARRO, R. ACEVES, M. C. VARGAS and C. Z. MENEZES, *J. Appl. Phys.* **58** (1985) 2066.
13. PAUL M. RACCAH, J. W. GARLAND, Z. ZHANG, H. M. AMY, J. RENO, T. K. SOU, M. BOUKERCHE and J. P. FAURIE, *J. Vac. Sci. Technol.* **A4** (1986) 2077.
14. E. GALVÃO DA SILVA, R. B. SCORZELLI, F. SANCHEZ-SINENCIO, OCTAVIO ALVAREZ-F. and J. G. MENDOZA-ALVAREZ, *J. Appl. Phys.* to be published.
15. N. V. JOSHI and L. MOGOLLÓN, *Prog. Cryst. Growth Charact.* **10** (1985) 65.

Received 2 February
and accepted 13 June 1988